

# HIGH BETA CAVITY OPTIMIZATION FOR ISAC-II

R.E. Laxdal and V. Zvyagintsev, TRIUMF, Vancouver, Canada  
 Z.H. Peng, CIAE, China Institute of Atomic Energy, Beijing, China

## Abstract

The linac for ISAC-II comprises twenty cavities of medium  $\beta$  quarter wave cavities now in the production phase. A second stage will see the installation of  $\sim 20$  MV of high  $\beta$  quarter wave cavities. The cavity structure choice depends on the efficiency of operation, cost, stability, beam dynamics and schedule. Two main cavity types are considered; a low frequency 106 MHz option and a high frequency 141 MHz cavity. We compare and contrast the cavity choices.

## INTRODUCTION

TRIUMF is now constructing an extension to the ISAC facility, ISAC-II, [1], to permit acceleration of radioactive ion beams up to energies of at least 6.5 MeV/u for masses up to 150. Central to the upgrade is the installation of a heavy ion superconducting linac designed to accelerate ions of  $A/q \leq 7$  to the final energy. The superconducting linac is composed of two-gap, bulk niobium, quarter wave rf cavities, for acceleration, and superconducting solenoids, for periodic transverse focussing, housed in several cryomodules. The cryomodules are grouped into low, medium and high beta sections corresponding to cavities with optimum velocities of  $\beta_o = 4.2\%$ ,  $\beta_o = 5.8, 7.1\%$  and  $\beta_o = 10.4\%$  respectively.

Due to experimental pressure and budget limitations the installation of the linac has been grouped into three stages highlighted in Fig. 1. The initial Stage 0 to be completed in 2005 includes the installation of a transfer line from the ISAC DTL ( $E = 1.5$  MeV/u) and the medium beta section to produce 18 MV of accelerating voltage for initial experiments. Stage 1 to be completed two years later includes the installation of the three high beta modules for a further 18 MV. The ISAC-II accelerator final Stage 2 is foreseen for 2010. The twenty medium beta cavities are installed four per cryomodule in a total of five modules now in production. The design effort on the high beta section is now intensifying.

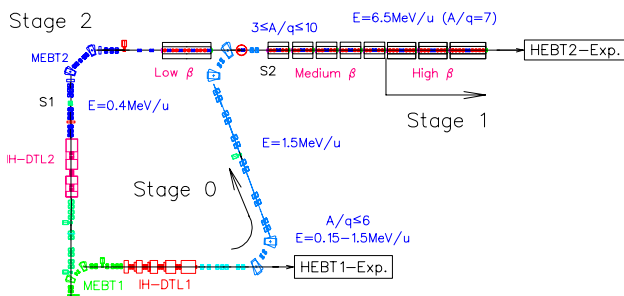


Figure 1: Stages 0, 1 and 2 for the ISAC-II upgrade.

## CAVITY VARIANTS

Three cavity variants are considered and shown in Fig. 2. The benchmark cavity, (a) *round141*, has identical transverse dimensions to the medium beta cavity[2] but is designed as a 141 MHz cavity by shortening the overall length and adjusting the gap. In a second variant, (c) *round106*, the cavity frequency is kept at 106 MHz but the cavity transverse dimensions are scaled to increase the beta from 7.1% to 10.4%. The quadrupole asymmetry in the accelerating fields [3] is somewhat larger in the high frequency case by virtue of the smaller inner conductor. A third variant, (b) *flat141*, is also considered where the 141 MHz cavity inner conductor is flattened near the beam ports to produce a smaller quadrupole asymmetry. This variant has a lower optimum beta, 9%, suitable for use in the beginning of the high beta section.

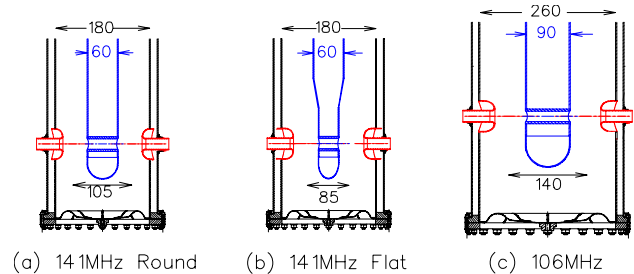


Figure 2: Three cavity variants considered in the study.

## BEAM DYNAMICS

The field asymmetries from the three models are summarized in Fig. 3 over the operating velocity range required of the cavity for an accelerating gradient of 6 MV/m, an ion of  $A/q = 3$ , and a phase of  $\phi_s = -30^\circ$ . Shown are the corrected vertical steering components and the vertical and horizontal defocussing perturbations for a 1 mm displacement from the electrical axis. The dipole steering components can be reduced to less than 0.1 mrad over the whole velocity range, for even the lightest beams, by shifting the cavities down by 1.3, 1.0 and 2 mm respectively for the *round141*, *flat141* and *round106* cases with respect to the beam and solenoid axis. In particular the beam port position with respect to the inner conductor tip is varied to reduce the required shift and minimize the steering effect.

## Linac Variants

The beam dynamics of the three cavity types are studied in three linac variants. The benchmark variant consists of twenty 141 MHz high beta cavities divided into two modules of six cavities and one module of eight cavities with one solenoid in each module. In a second vari-

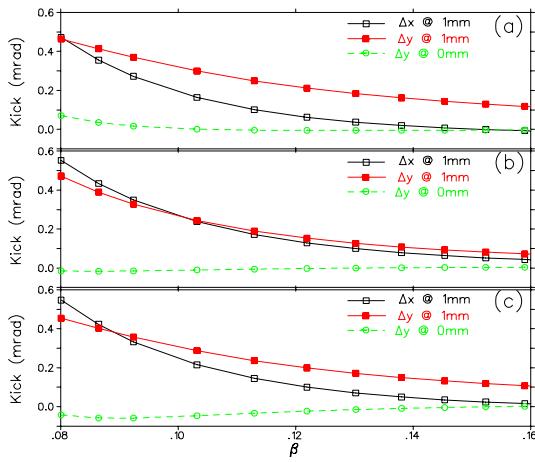


Figure 3: Focussing and steering perturbations for the three cavity geometries (a) *round141* (b) *flat141* (c) *round106* as calculated in LANA based on HFSS fields. Shown are the corrected vertical steering components (dashed lines) and the vertical and horizontal defocussing perturbations for a 1 mm displacement from the electrical axis.

ant the six cavities in the first high beta module are replaced with the flat 141 MHz cavities to reduce the impact of the quadrupole asymmetry. In the last variant fourteen 106 MHz cavities are used divided into two modules of four cavities and one module of six cavities. A plot of accelerator efficiency as a function of particle  $A/q$  values is given in Fig. 4. All variants give an overall efficiency of 80% for light ions and 90% for heavy ions as compared to the optimum efficiency (accelerating always at  $\beta_o$ ).

A summary of the beam dynamics calculations for the Stage 1 linac using the three linac variants is given in Fig. 5 and Fig. 6. Given are the transverse beam envelopes and the beam centroids. In each case a single charge state beam with initial emittance of  $1.8\pi\text{mm-mr}$  and  $12\pi\text{keV/u-n}$ s (ten times the expected emittances) is simulated. The large beam is used to characterise differences in the effective dynamic aperture of the three variants. Also shown

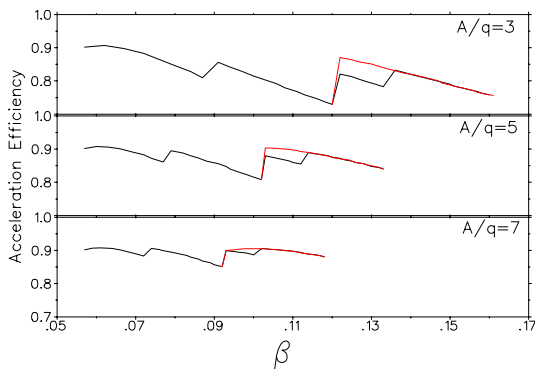


Figure 4: The acceleration efficiency for various  $A/q$  values for the Stage 1 linac for the benchmark case and for the first six high beta cavities replaced by the *flat141* cavity.

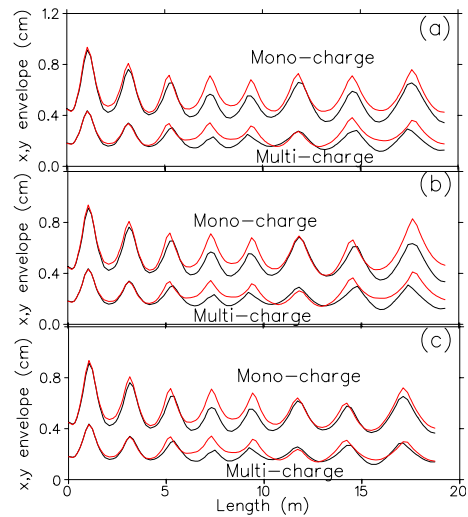


Figure 5: The transverse beam envelopes as a function of longitudinal position along the medium and high beta sections for (a) *round141* (b) *flat141/round141* variant (c) *round106* variant. In each case a single charge state beam with initial emittance of  $1.8\pi\text{mm-mr}$  and  $12\pi\text{keV/u-n}$ s (ten times the expected emittances) is simulated. Also shown is a multi-charge beam ( $\Delta Q/Q = \pm 5\%$ ) with initial emittances of  $0.3\pi\text{mm-mr}$  and  $2.\pi\text{keV/u-n}$ s.

are results for a multi-charge beam with initial emittances of  $0.3\pi\text{mm-mr}$  and  $2.\pi\text{keV/u-n}$ s. The reduced quadrupole asymmetry in the *round106* cavity results in less asymmetry in the transverse envelope compared to the other two 141 MHz variants. However the transverse and longitudinal emittance growth for the three cases are virtually identical. The beam centroid shifts are tolerably small in all cases.

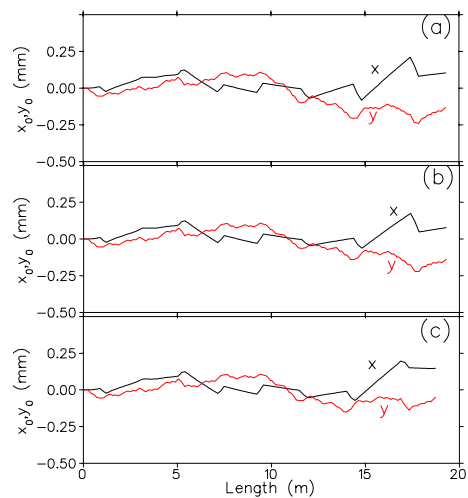


Figure 6: The transverse beam centroids as a function of longitudinal position along the medium and high beta sections for (a) *round141* (b) *flat141/round141* variant (c) *round106* variant.

## RF CHARACTERISTICS

The rf parameters of the three cavity variants are given in Table 1. The cavity rf properties are simulated in HFSS.

Table 1: Parameters of cavity variants

Parameter	<i>round141</i>	<i>flat141</i>	<i>round106</i>
f (MHz)	141.4	141.4	106.1
$\beta_o$	0.104	0.09	0.103
TTF <sub>o</sub>	0.089	0.086	0.093
bore (mm)	20	20	20
gap (mm)	45	45	50
drift tube (mm)	60	40	90
$L_{eff}$ (mm)	180	180	260
Height (mm)	577	577	737
$\Delta y$ (mm)	1.3	1.0	2.0
$f_{mech}$ (Hz)	150	150	134
$E_a$ (MV/m)	6	6	6
V (MV)@6MV/m	1.08	1.08	1.56
$E_p/E_a$	4.7	5.6	4.6
$B_p/E_a$ (mT/MV/m)	10.3	10.5	9.9
$U/E_a^2$ (J/(MV/m) <sup>2</sup> )	0.073	0.078	0.194
$R_s Q_0$ ( $\Omega$ )	24.8	24.9	26.8
$R_{sh}/Q$ ( $\Omega$ )	499	470	521

We compare all cavities at a gradient of 6 MV/m calculated over the cavity length defined as the inside diameter of the outer rf surface. There is little difference between the two 141 MHz variants except for the higher peak surface field in the *flat141* variant. Instead we concentrate here on the comparison of the *round141* and the *round106* variants. Due to the increased voltage the main practical difference is that fewer sub-systems (14 as compared to 20) would be required for the lower frequency. However due to the higher stored energy and somewhat higher  $Q_0$  (see below) more power is required to provide a sufficient tuning bandwidth.

Let us examine the role of rf frequency in cavity scaling. The surface resistance is given by

$$R_s = R_{BCS} + R_{mag} + R_0$$

where

$$R_{BCS} = 2 \times 10^{-4} \frac{1}{T} \left( \frac{f}{1.5} \right)^2 e^{-17.7/T}$$

and

$$R_{mag} = 0.3n\Omega \cdot H_{ext}(mOe) \sqrt{f(GHz)}$$

Results of these expressions are shown in Table 2 assuming a magnetic field attenuation factor of five from the earth's field. The TRIUMF medium beta cavity has a typical  $Q$  of  $1.5 \times 10^9$  at low field that droops to  $5 \times 10^8$  at a gradient of 6 MV/m. Since  $R_s Q = 19\Omega$  for this cavity this corresponds to surface resistance values of 12.7 and 38.2 n $\Omega$ . Assuming  $R_0$  is independent of frequency we can estimate that the high-field surface resistance for the 141 MHz cavity is enhanced due to the increased values of  $R_{BCS}$  and

$R_{mag}$  to be 42.5 n $\Omega$  an increase of 11%. Using these values of  $R_s$  and the tabulated values of  $R_s Q_0$  gives expected  $Q_0$  values of  $5.8 \times 10^8$  and  $7 \times 10^8$  respectively for the *round141* and *round106* cavity respectively. The cavity power dissipation,  $P_{cav} = \omega_o U / Q_0$ , is listed in Table2.

Table 2: Frequency dependence of surface resistance and cavity power

f (MHz)	106	141
$R_{BCS}$ (n $\Omega$ )	3.5	6.3
$R_{mag}$ (n $\Omega$ )	9.8	11.3
$R_0$ (n $\Omega$ )	25	25
$R_s$ (n $\Omega$ )	38.2	42.5
$Q_0$ @6MV/m	$7 \times 10^8$	$5.8 \times 10^8$
$P_{cav}$ (W)@6MV/m	6.7	4.2
$\beta$	280	230
$P_{amp}$ (W)@6MV/m	1200	620

The increased quality factor of the 106 MHz cavity increases the amount of overcoupling required to achieve a specified rf bandwidth (in our case  $\Delta f/f = 4 \times 10^{-7}$ ). The forward power can be calculated from the coupling factor,  $\beta$ , and the cavity power using  $P_f = P_{cav} * (\beta + 1)^2 / (4\beta)$ . To provide for the bandwidth the peak amplifier power must be sufficient to deliver twice the required forward power after considering the line losses. These deliberations lead us to estimating that the required amplifier would be almost a factor of two larger in the 106 MHz case.

## CONCLUSION

There is no strong beam dynamics argument to choose one variant over another. The total dissipated cavity power is 17% less in the high frequency cavity and the total amplifier power is 29% less. The high frequency cavity is also somewhat more mechanically stable. These advantages are not sufficient to force a cavity choice. The two most compelling arguments are that the design time for the 141 MHz cavity and ancillaries will be significantly less. This is balanced somewhat by the attractiveness of reducing the number of sub-systems by adopting the lower frequency. The final choice will be based on a review of the schedule and cash flow.

## ACKNOWLEDGEMENT

The authors would like to thank R. Eichhorn for useful discussions and D. Gorelov for help with LANA.

## REFERENCES

- [1] P. Schmor, et al, "Development and Future Plans at ISAC", this conference.
- [2] A. Facco, et al, "The Superconducting Medium  $\beta$  Prototype for Radioactive Beam Acceleration at TRIUMF", PAC2001, Chicago, June 2001.
- [3] M. Pasini, et al, *Beam Dynamics Studies on the ISAC-II Post Accelerator at TRIUMF*, EPAC2002, Paris.